ORIGINAL ARTICLE

DOI: 10.4274/hamidiyemedj.galenos.2024.19870

Hamidiye Med J 2024;5(1):29-36

Morphometric and Clinical Importance of Anatomical Structures Related to Fossa Cerebellaris in Surgical Approaches

Fossa Cerebellaris'te Bulunan Anatomik Yapıların Cerrahi Yaklaşımlardaki Morfometrik ve Klinik Önemi

Mehmet Ozan Durmaz[1], Mehmet Can Ezgü[1], Nuket Göçmen Karabekir[2]

[1]*University of Health Sciences Türkiye, Gülhane Training and Research Hospital, Clinic of Neurosurgery, Ankara, Türkiye*

[2]*Dokuz Eylül University Faculty of Medicine, Department of Anatomy, İzmir, Türkiye*

ABSTRACT

Background: Surgical approaches to the posterior fossa are always challenging and complex anatomical structures pose risks for the removal of cerebellar lesions. In this study, we aimed to define a safe corridor for tumor surgery for neurosurgeons by examining the anatomy of the fossa cerebellaris in detail and measuring some osseous landmarks.

Materials and Methods: In this study, 15 dry bone craniums and 8 cadavers were morphometrically examined and the distances between some important bony landmarks were measured with a digital caliper with millimeter precision. The measurements were compared using statistical methods.

Results: The distance between anterior margin of foramen magnum (FM) and spheno-occipital synchondrosis (SOS) was found to be longer in dry skull than in cadaver measurements, and a statistically significant difference was found. There was no significant difference between right and left side comparisons for for. jugulare, for. magnum, porus acousticus internus and canalis nervi hypolossi in both dry skull and cadaver samples.

Conclusion: Longer distance between the anterior border of FM and SOS make difficult the surgical approach to the clivus lesions, but facilitate to the reach the anterior FM tumors. Careful preoperative evaluation of this distance provides good anatomical knowledge for neurosurgeons dealing with such lesions.

Keywords: Posterior fossa, tumor, spheno-occipital synchondrosis, anatomy

ÖZ

Amaç: Posterior fossaya cerrahi yaklaşımlar her zaman zorlayıcı olmuştur ve karmaşık anatomik yapılar, serebellar lezyonların eksizyonu ameliyatlarında risk oluşturmaktadır. Bu çalışmada, fossa cerebellarisin anatomisi ayrıntılı olarak incelenerek ve bazı osseoz işaretler ölçülerek beyin cerrahlarına tümor cerrahisi için güvenli bir koridor tanımlamak amaçlandı.

Gereç ve Yöntemler: Bu çalışmada 15 kuru kemik kranyum ve 8 kadavra morfometrik olarak incelendi ve bazı önemli kemiksel işaretler arasındaki mesafeler milimetre hassasiyetinde bir dijital kumpasla ölçüldü. Ölçümler istatistiksel yöntemler kullanılarak karşılaştırıldı.

Bulgular: Foramen magnum'un (FM) ön kenarı ile sfeno-oksipital sinkondroz (SOS) arasındaki mesafe kuru kafatası ölçümlerinde kadavra ölçümlerine göre daha uzun bulunmuş ve istatistiksel olarak anlamlı bir fark tespit edilmiştir. Hem kuru kafatası hem de kadavra örneklerinde for. jugulare, for. magnum, porus acousticus internus ve canalis nervi hypolossi için sağ ve sol taraf karşılaştırmaları arasında anlamlı bir fark bulunmamıştır.

Sonuç: FM'nin ön sınırı ile SOS arasındaki mesafenin uzun olması klivus lezyonlarına cerrahi yaklaşımı zorlaştırırken, anterior FM tümörlerine ulaşmayı kolaylaştırır. Bu mesafenin ameliyat öncesi dikkatli bir şekilde değerlendirilmesi, bu tür lezyonlarla uğraşan beyin cerrahları için iyi bir anatomik bilgi sağlamaktadır.

Anahtar Kelimeler: Posterior fossa, tümör, sfeno-oksipital sinkondroz, anatomi

Address for Correspondence: Mehmet Can Ezgü, University of Health Sciences Türkiye, Gülhane Training and Research Hospital, Clinic of Neurosurgery, Ankara, Türkiye
Phone: +90 555 714 34 87 E-mail: mcanezgu@gmail.com **ORCID ID:** orcid.org/0000-0001-7537-0055

Received: 19.01.2024 **Accepted:** 14.02.2024

Introduction

The fossa cerebellaris is located in the fossa crane posterior. Fossa cranii posterior is surrounded by the clivus and dorsum sellae anteriorly, the pars petrosa and pars mastoidea of the temporal bone laterally, and the occipital bone and angulus mastoideus of the parietal bone posteriorly. It contains the occipital lobe, cerebellum, and related anatomical structures (1). The fossa crane posterior is the deepest and largest fossa of the cranium. Important osseous structures in this region are the foramen magnum (FM), meatus acousticus internus, foramen jugulare (FJ), canalis nervi hypoglossi, canalis condylaris, sulcus sinus petrosi inferioris, sulcus sinus transversi, sulcus sinus sigmoidei, protuberantia occipitalis interna, and dorsum sellae. During surgical approaches to posterior fossa lesions, these structures pose some risks for neurosurgeons and require special attention. Injuries to these delicate anatomical structures may result in catastrophic outcomes (2).

In this study, we plan to examine the osseous anatomy and neighborhood and distance relations of the region, which are important for surgical interventions to the fossa cerebellaris [pathologies of the cerebellum, for. magnum and upper cervical region pathologies and congenital malformations of this region, schwannoma-like pathologies localized to the meatus acusticus, pathologies such as glomus jugulare involving the jugular foramen (JF), etc.]. Some morphometric measurements were performed, and the results were compared with those reported in the relevant literature.

Materials and Methods

In this study, following the approval of the Dokuz Eylül University Non-Invasive Research Ethics Committee (no: 2012/22-8, date: 21/06/2012) we morphometrically examined the osseous structures in 15 dry bone cranium and 8 cadavers, which can be measured with a maximum of 3 mm deficiencies, in the Dokuz Eylül University Faculty of Medicine Anatomy Department Laboratory.

All measurements were recorded with a digital caliper, accurate to millimeters. Measurements made on dry bones and cadavers are listed separately in the table. The results of the right and left comparisons and reciprocal comparisons of the measurements made separately (cadaver-dry bone) within their group were statistically analyzed. None of the skulls and cadavers examined showed signs of previous cranial surgery, malformation, or trauma. All samples were photographed using a Canon EOS 700D (55 mm lens) camera.

Important anatomical foramens, passages, and clinically related structures in this fossa and its neighbors; the measurable distances in dry bone and cadaver, and the distances that may be of clinical (application area) importance were measured (Figures 1, 2, 3).

Parameters that can be measured on dry bone (right/left); FM anterior-posterior length, FM transverse length, porus acusticus internus (PAI) superior-inferior diameter, PAI anterior-posterior diameter, FJ superior-inferior diameter, FJ mediolateral diameter, PAI lower edge, the distance between the upper edge of the FJ, the distance between the lower edge of the FJ and the canalis nervi hypolossi (CNH), the distance between the anterior border of the CNH-FM, the distance from the PAI-sinus transversus (ST)-sinus sigmoideus (SS) junction, the posterior edge of the FJ-ST and SS junction, and ST and SS junction-protuberentia occipitalis interna (POI) were measured.

Parameters measured on dry bone and cadaver are, respectively, as right/left distance; distance between PAIs and midline, distance between FJs and midline, distance between CNHs and midline, distance between FM posterior border and POI, and between FM anterior border-spheno-occipital synchondrosis (SOS) joint distance was measured.

The distance of the ST-SS junction to the midline was measured as the right/left distance of the parameters measured on the cadaver.

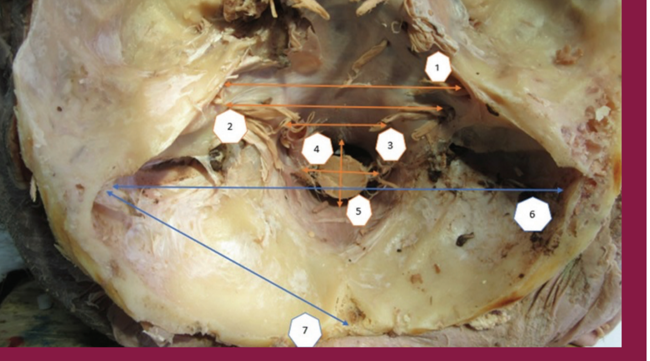

Figure 1. Measurement distances
1. Distances between the porus acousticus internus and distances to the midline
2. Distances between the foramen jugulares and distances to the midline
3. Distances between the canalis nerve hypoglossies and distances to the midline
4. Foramen magnum (FM) transverse length
5. FM anteroposterior length
6. Distance between the midline and the junction of the transversus-sigmoid sinus
7. Distance between the protuberantia occipital interna and the junction of the transversus-sigmoid sinus

Statistical Analysis

SPSS version 15.0 (Statistical Package for the Social Sciences Inc., Chicago, IL, USA) was used to evaluate the data. The obtained values are shown as mean ± standard deviation or median (minimum-maximum) where appropriate. Examination of normal distribution assumptions for continuous data was evaluated using QQ plots, histograms, and the Shapiro-Wilk test. Normally distributed variables were analyzed using Student's t-test, and non-normally distributed variables were analyzed using the Mann-Whitney U test. Paired t-test or Wilcoxon signed-rank test was used to compare the differences between the measurements made separately in the same dry bone and cadaver for the right and left sides depending on the data distribution. The level of significance was set as $p<0.05$ in all statistical analyses. Because our research was a cadaveric study, patient consent could not be obtained.

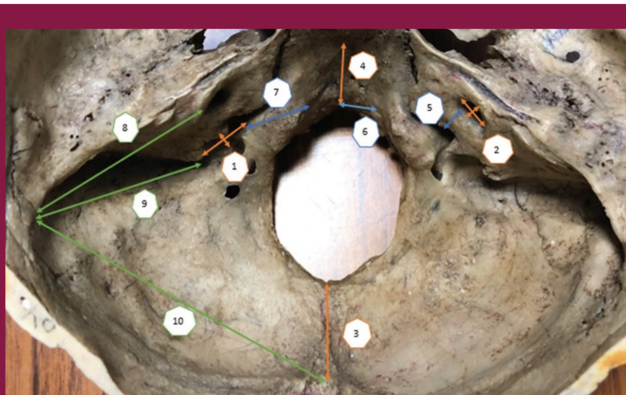

Figure 2. Some posterior fossa measurement distances in the dry skull
1. Superior-inferior and mediolateral diameters of the foramen jugulare (FJ)
2. Superior-inferior and anteroposterior diameters of the porus acousticus internus
3. Distance between the posterior margin of the foramen magnum (FM) and the protuberantia occipital interna
4. Distance between the anterior margin of the FM and spheno-occipital synchondrosis
5. Distance between the inferior margin of the porus acousticus internus and the superior margin of the FJ
6. Distance between the superior margin of the FM and canalis nervi hypoglossi
7. Distance between the inferior margin of the FJ and canalis nervi hypoglossi
8. Distance between the porus acousticus internus and the junction of the transversus-sigmoid sinus
9. Distance between the posterior margin of the FJ and the junction of the transversus-sigmoid sinus
10. Distance between the protuberantia occipital interna and the junction of the transversus-sigmoid sinus

Results

According to the analysis results of the data obtained from 15 dry bones;

The mean magnum anterior-posterior length was measured as 34.3±2.55 mm; the mean magnum transverse length was measured as 27.9±3.27 mm. Anteroposterior (AP) diameter/transverse diameter was defined as FM index 8, and 9 dry bones (60%) were observed as FMI >1.2 and were defined as ovoid-shaped.

PAI superior-inferior diameter, right/left mean=2.59±1.12 mm/2.85±1.35 mm; the anterior-posterior diameter of the PAI was measured as right/left mean=3.78±1.35 mm/4.43±1.49 mm. For. jugulare superior-inferior diameter, right/left mean=5.47±1.15 mm/5.88±1.50 mm; for. jugulare mediolateral diameter was measured as right/left mean: 10.9±2.37 mm/11.1±2.29 mm. The distance between the

Figure 3. Measurement of distances between the porus acousticus internus and foramen jugulares using a digital caliper

upper edge of the for. jugulate was measured as the right/left mean=6.0±0.76 mm/6.02±0.71 mm. The distance between the lower edge of the for. jugulare and the hypoglossi of the canalis nerve was measured as the right/left mean=9.47±1.39 mm/9.5±1.40 mm. The distance between the anterior border of the for. magnum was measured as the right/left mean=9.86±1.65 mm/9.8±1.60 mm.

The distance from the PAI to the ST and SS junction right/left mean=30.9±4.30 mm/31.04±4.42 mm, the distance from the posterior edge of the jugulare to the ST and SS junction right/left mean=31.7±4.27 mm/31.8±4.18 mm, and the distance from the sinus trasversus and SS junction to the POI right/left mean=31.9±1.60 mm/32±1.79 mm.

The distance between the right and left PAI dry bone cadaver (mean=48.8±4.70 mm/53.2±6.85 mm), the distance between the right and left FJ dry bone cadaver (mean=51.1±2.54 mm/48.7±6.84 mm), and the distance between the right and left canalis nervi hypoglossis were measured as dry bone cadaver (mean=26.7±2.02 mm/23.2±3.53 mm).

The distance between posterior border of for. magnum and protuberantia occipitalis interna dry bone cadaver (mean=40.5±5.76 mm/46.4±9.90 mm), and the distance between anterior border of for. magnum and SOS was measured as dry bone cadaver (mean=19.2±4.42 mm/11.9±2.47 mm).

PAI distance from the midline to the right (dry bone 24.4±2.37 mm; cadaver 26.2±3.34 mm), PAI distance from the midline to the left (dry bone 24.4±2.37 mm; cadaver 26.8±3.50 mm), distance of for. jugulares from the midline to the right (dry bone 25.5±1.26 mm; cadaver 24.2±3.47 mm), for. jugulares distance from the midline to the left (dry bone 25.5±1.27 mm; cadaver 24.5±3.43 mm), canalis nervi hypoglossi distance from the midline to the right (dry bone 14.3±2.97 mm; cadaver 11.5±1.59 mm), and canalis nervi hypoglossi distance from the midline to the left (dry bone 14.4±2.88 mm; cadaver 11.7±2.01 mm).

For the right and left sides, when the paired t-test or Wilcoxon signed-row test, sample t-test results were analyzed to compare the differences between the measurements made separately in the same dry bone and cadaver, the results obtained are shown in Tables 1, 2, 3.

In comparative analyses, only the distance between the FM anterior border and SOS was found to be longer in dry

Table 1. Comparison of measurements between the dry skull and cadavers

Measurement/mm	Material	Mean	SD	Median	p-value
Distance between the right and left porus acusticus internus	Dry skull	48.8	4.70	50.3	0.080
	Cadaver	53.2	6.85	54.0	
Distance between the right and left foramen jugularis	Dry skull	51.1	2.54	51.3	0.226
	Cadaver	48.7	6.84	49.5	
Distance between the right and left canalis nervi hypoglossi	Dry skull	26.7	2.02	26.9	0.006
	Cadaver	23.2	3.53	22.1	
Distance between the posterior margin of for. magnum area snr and the protuberantia occipitalis interna	Dry skull	40.5	5.76	39.2	0.083
	Cadaver	46.4	9.90	47.5	
Distance between the anterior margin of the for. magnum and spheno-occipital synchondrosis	Dry skull	19.2	4.42	18.2	<0.001
	Cadaver	11.9	2.47	12.1	
Distance between porus acusticus internus and midline (Right)	Dry skull	24.4	2.37	25.1	0.149
	Cadaver	26.2	3.34	26.8	
Distance between porus acusticus internus and midline (Left)	Dry skull	24.4	2.37	25.1	0.064
	Cadaver	26.8	3.50	26.3	
Distance between the foramen jugulate and midline (Right)	Dry skull	25.5	1.26	25.8	0.202
	Cadaver	24.2	3.47	24.8	
Distance between the foramen jugulate and midline (Left)	Dry skull	25.5	1.27	25.9	0.308
	Cadaver	24.5	3.43	24.6	
Distance between the canalis nerve hypoglossi and midline (Right)	Dry skull	14.3	2.97	13.4	0.021
	Cadaver	11.5	1.59	11.4	
Distance between the canalis nervi hypoglossi and midline (Left)	Dry skull	14.4	2.88	13.8	0.030
	Cadaver	11.7	2.01	10.8	

SD: Standard deviation

Table 2. Comparison of right-left side measurements performed in the dry skull		
Measurement	**T-statistic**	**p-value**
Superior-inferior diameter of the porus acousticus internus	-1.476	0.162
Anteroposterior diameter of the porus acousticus internus	-2.785	0.015
Superior-inferior diameter of the foramen jugulate	-1.678	0.116
Mediolateral diameter of the foramen jugulate	-0.799	0.438
Distance between inferior margin of porus acousticus internus and superior margin of foramen jugulare	0.923	0.372
Distance between the inferior margin of the foramen jugulare and canalis nerve hypoglossi	-0.541	0.597
Distance between canalis nerve hypoglossi and anterior margin of the foramen magnum	0.888	0.389
Distance between porus acousticus internus and junction of sinus transversus sinus sigmoideus	-0.961	0.353
Distance between the posterior margin of the Foramen jugulare and the junction of the sinus transversus sinus sigmoideus	-1.642	0.123
Distance between porus acousticus internus and midline	-0.700	0.635
Distance between foramen jugulare and midline	-0.947	0.756
Distance between canalis nervi hypoglossi and midline	-0.798	0.719
Distance between protuberentia occipitalis interna and junction of sinus transversus sinus sigmoideus	-1.002	0.333

Table 3. Comparison of right-left side measurements performed on the cadaver		
Measurement	**T-statistic**	**p-value**
Distance between porus acousticus internus and midline	-1.248	0.252
Distance between foramen jugulare and midline	-1.042	0.332
Distance between canalis nervi hypoglossi and midline	-0.757	0.474
Distance between the junction of the sinus transversus sinus sigmoideus and the midline	-0.717	0.497

bone than in cadaver measurements, and a statistically significant difference was found (p<). The reason for this was evaluated as SOS is quite evident in some materials, but it is more difficult to detect in cadaver samples than in dry bone. There was no significant difference between the right and left side comparisons in both dry bone and cadaver samples.

Discussion

The area between the cerebellum, pons, and pyramid and filled by the pontocereballaris system is the region that should be evaluated clinically because of primary or metastatic tumor formations. Cerebellar metastases constitute only 10-15% of brain metastases, and approximately 31-32% of these metastases are single metastases. Cerebellar metastases are grouped as life-threatening lesions compared with metastases located in other parts of the brain. They can cause hydrocephalus, irreversible brainstem compression, and herniation of posterior fossa structures (such as tonsils) up and down (through the FM) (2). VII, IX, X, Xl, XII. cranial nerves, a. vertebralis, and v. petrosa are located in this region (3).

Surgically, this area can be accessed via the occipital, temporal, pyramidal, and translabyrinthine routes. The accessorius system crosses the pontocerebellar and emerges from the pars nervosa of the FJ. N. hypoglossus leaves the medulla oblongata with a more internal course between the pyramid and oliva. Its exit from the canalis hypoglossi is more basal and somewhat sheltered. The exit points of the petrosa are lateral to the superior vesinus petrosus in the medulla oblongata.

During the operation, from the occipital to the upper n. vestibularies, n. facialis is seen to occur deeper. The facial nerve leads to the PAI. More basally, n. cochlearis and in between them, n. intermediateus is found in a more hidden position. All these nerve structures are covered by the arachnoid membrane. The vasa labyrinth accompanies these nerve structures. Following the pontocerebellar junction on both sides, n. trigeminus tends anteriorly in the sagittal direction and is observed as a structure that can be encountered in the pontocerebellar region.

The cisternal part of n. trigeminus protrudes bilaterally from the anterior aspect (anterior-lateral part) of the pons. When the exit site is carefully examined, a small motor root (radix motoria) and a large sensory root (radix sensoria) stand out. N. trigeminus leaves the fossa cranii posterior and moves forward (4,5,6). Around the for. magnum, there is the sulcus sinus marginalis, right next to the crista occipitalis interna, i.e., the sulcus sinus occipitalis. For. magnum is surrounded by the sinus marginalis. There are anastomoses to the vertebral veins, v. cervicalis profunda, and sinus occipitalis. A. vertebralis enters the region over the atlas by passing the membrane atlanta-accipitalis. The flocculus and tonsils of the cerebellum are in a topographically close relationship with the for. magnum. Because of sudden changes in cerebrospinal fluid compression or pressure caused by tumors, the posterior tracts of the medulla oblongata, tonsils, and n. The ascending spinal cord of the accessorius is significantly affected (3,6).

It is important to evaluate the anatomical structure of the patient to determine the surgical access and technique for surgical interventions for the fossa cerebellaris and its neighbors. For surgical approaches of this region, the magnum has special importance and value. For. magnum's anterior-posterior and transverse diameters can change the shape of the surgical approach. Also flat or ovoid for. magnum may cause early symptomatization of pathologies of this region such as Chiari malformations and basilar invagination. Anatomical morphological studies and three-dimensional radiology studies of this region make surgical interventions for regional pathologies safer.

Cerebellopontine angle tumors are the most common tumors in the posterior fossa cranii. Most of them are benign and approximately 80% of them are vestibular schwannomas, although they can be observed in meningiomas, subgroup cranial nerve schwannomas, and epidermoid tumors (7,8). Three pairs of cerebellar arteries are associated with certain neural structures during their course. Each artery is associated with a cerebellar surface, cranial nerve, and fissure. This rule was proposed by Rhoton (9) to simplify the surgical corridor, craniotomy, and cerebellar retraction.

Natsis et al. (10) evaluated the diameters of the occipital condyle and FM in 143 dry bones in a Greek population in 2013 and found the FM AP length as 35.53±3.06 mm and the FM transverse length as 30.31±2.79 mm. In our measurements, the mean FM AP length was measured as 34.3±2.55 mm; the mean FM transverse length was evaluated as 27.9±3.27 mm and was considered consistent with many morphometric studies in the literature. In the same study, they divided the for. magnum structure into 7 shapes and especially emphasized that the shape of the FM is important in terms of approaching the lesions in the ventral for. magnum (10).

Wanebo and Chicoine (11), in 32 cranial and 6 cadavers in whom they evaluated transcondylar approaches to FM, stated that longer FM AP diameters resulted in a wider contralateral visual angle after condylar bone resection. Manoel et al. (12) examined FM morphometry in 215 dry bones and stated that there were morphometric differences in terms of ethnicity and gender, but there was no morphological difference, as in some other studies. There are many studies in the literature on FM morphometry in line with gender and ethnic characteristics.

Avci et al. (13) evaluated FM diameters and shapes in 30 skulls and 10 cadavers; they measured the mean AP diameters as 34.5 mm and the transverse diameters as 29 mm. They also defined the AP diameter/transverse diameter as the FM index and defined FMI >1.2 as FM with an ovoid shape. They also stated that surgical exposure of the anterior part of ovoid-shaped FM may be more difficult (13). Our dry bone measurements were also evaluated in accordance with the literature on the lengths of FM diameters. It was defined as 1.2< and ovoid shaped in 9 (60%) of the FMI materials.

Gupta et al. (14), in a morphometric study of the JF in 50 dry bones, measured the mean mediolateral length as 13.25±1.56 and 12.26±1.33 mm on the right and left, respectively, which is similar to our measurements. Das et al. (15), in their extensive morphometric studies for JF, determined the AMW diameters as 4.34-5 mm, right/left respectively, and PLW 7.07-5.51 mm, respectively. Our measurements were determined as 5.47-5.88 mm, right/left, respectively, and they are similar.

Matsushima et al. (16), in laboratory studies where they evaluated the surgical anatomical limitations of the retrosigmoid approach for suprajugular localized pathologies, suggested that retrosigmoid or condylar approaches can be preferred in the approach to intracranially located jugular pathologies (9,17); however, they reported that residual lesions may remain in lesions located or extending in the upper part of the JF (18). Our study is limited as it only evaluates the intracranial section for JF, and there are many surgical approaches (infratemporal, transcondylar, suboccipital, retrosigmoid, etc.) that will be able to recommend the use of a standard technique or combined techniques to evaluate the width of the surgical field with morphometric studies for the structure.

Sekerci et al. (19) evaluated the PAI and examined 120 dry temporal bones, evaluated PAI in terms of ethnicity, diameters, and shapes, and measured superior-inferior diameter of 4.31±0.88 mm and anterior-posterior diameter of 6.64±0.94 mm, respectively. Özandaç et al. (20) evaluated meatus acusticus internus (MAI) as 2.3-5.7 mm and 3.1-7.7 mm, respectively, in their radiological studies. In our study, the superior-inferior diameter of the PAI was measured as right/left mean=2.59±1.12 mm/2.85±1.35 mm. The anterior-posterior diameter of the PAI was measured as right/left mean=3.78±1.35 mm/4.43±1.49 mm.

Akın-Saygin et al. (21), in their study where they evaluated the MAI morphometry on 166 temporal dry bone, found the mean distance of MAI to JF as 6.15±1.37 mm /6.19±1.55

mm on the right and left, respectively, and their findings are consistent with our measurements. Kolagi et al. (22), in their anatomical morphometric studies, in which they evaluated the suboccipital retrosigmoid approach in 224 dry bones, the mean right/left distance between the uppermost part of the SS and the outermost part of the PAI, respectively; they evaluated it as 38.94 mm /38.09 mm (in the range of 32-44 mm). This is longer than our measurements (22).

The shortest distance between PAI and SS was reported by Bozbuğa et al. (23) and Day et al. (24) as an average of 31.1 mm and 34.5 mm, respectively. In our study, the distance between the PAI and the SS-ST junction was 30.9 mm on the right; it was measured as 31.04 mm on the left and was evaluated as similar to the results in the literature. These distances, especially in retrosigmoid approaches, are in the pre-surgical preparation phase; we believe that it will gain more importance with morphometric studies to reduce cerebellar retraction; however, it should be supported by radiological studies including three-dimensional angle measurements for this region.

Study Limitations

Our study was limited by the number of samples and evaluated only the foramen and intracranial region in relation to the measured parameters. There is a need for more anatomical studies in which the structure of this region is evaluated in three dimensions and each surgical approach technique is examined separately.

Conclusion

In surgical interventions for the fossa cerebellaris and adjacent structures at the posterior skull base, especially considering brain stem and pontocerebellar angle tumor surgical approaches, the evaluation of fossa cerebralis and fossa cerebellaris related structures, the locations of the neural foramen, and the pre-surgical evaluation of the three-dimensional structure of the FM, fossa cerebellaris, and posterior fossa are critical in terms of determining the surgical technique and planning a safe approach.

Ethics

Ethics Committee Approval: In this study, following the approval of the Dokuz Eylül University Non-Invasive Research Ethics Committee (no: 2012/22-8, date: 21/06/2012) we morphometrically examined the osseous structures in 15 dry bone cranium and 8 cadavers, which can be measured with a maximum of 3 mm deficiencies, in the Dokuz Eylül University Faculty of Medicine Anatomy Department Laboratory.

Informed Consent: Our research was a cadaveric study, patient consent could not be obtained.

Authorship Contributions

Surgical and Medical Practices: M.O.D, N.G.K., Concept: M.O.D, M.C.E., N.G.K., Design: M.O.D, M.C.E., N.G.K., Data Collection or Processing: M.O.D, M.C.E., N.G.K., Analysis or Interpretation: M.O.D, M.C.E., N.G.K., Literature Search: M.O.D, M.C.E., N.G.K., Writing: M.O.D, M.C.E., N.G.K.

Conflict of Interest: No conflict of interest was declared by the authors.

Financial Disclosure: The authors declared that this study received no financial support.

References

1. Arıncı K, Elhan A. Anatomi 1. Cilt, 4. Baskı, Güneş Kitapevi, Ankara 2006:55-57. [Crossref]
2. Sayyahmelli S, Tanrıverdi T. Posterior Fossa Metastazları. Türk Nöroşir Derg. 2017;27:93-97. [Crossref]
3. İkiz İ. Basis cranii interna›nın topografik anatomisi. Uludağ Üniv Tıp Fak Derg. 2000:55-59. [Crossref]
4. Canbolat AT. Nervus trigeminus kökünün pons seviyesinde nörovasküler komşulukları. İstanbul Üniversitesi Tıp Fak. Nöroşirurji AD, Uzmanlık tezi, 2398, İstanbul, 1981. [Crossref]
5. Yousry I, Moriggl B, Holtmannspoetter M, Schmid UD, Naidich TP, Yousry TA. Detailed anatomy of the motor and sensory roots of the trigeminal nerve and their neurovascular relationships: a magnetic resonance imaging study. J Neurosurg. 2004;101:427-434. [Crossref]
6. Rohen JW. Topographische anatomie. Shattauer Verlag, Stutgart, New York. 1973:24-29. [Crossref]
7. Samii M, Matthies C. Management of 1000 vestibular schwannomas (acoustic neuromas): Surgical management and results with an emphasis on complications and how to avoid them. Neurosurgery. 1997;40:11-23. [Crossref]
8. Sekhar LN, Jannetta PJ. Cerebellopontine angle meningiomas microsurgical excision and follow up results. J Neurosurg. 1984;60:500-505. [Crossref]
9. Rhoton AL Jr. The cerebellopontine angle and posterior fossa cranial nerves by the retrosigmoid approach. Neurosurgery. 2000;47:S93-129. [Crossref]
10. Natsis K, Piagkou M, Skotsimara G, Piagkos G, Skandalakis P. A morphometric anatomical and comparative study of the foramen magnum region in a Greek population. Surg Radiol Anat. 2013;35:925-934. [Crossref]
11. Wanebo JE, Chicoine MR. Quantitative analysis of the transcondylar approach to the foramen magnum. Neurosurgery. 2001;49:934-941. [Crossref]
12. Manoel C, Prado FB, Caria PHF, Groppo FC. Morphometric analysis of the foramen magnum in human skulls of Brazilian individuals: its relation to gender. Braz J Morphol Sci. 2009:26;104-108. [Crossref]
13. Avci E, Dagtekin A, Ozturk AH, Kara E, Ozturk NC, Uluc K, et al. Anatomical variations of the foramen magnum, occipital condyle and jugular tubercle. Turk Neurosurg. 2011;21:181-190. [Crossref]
14. Gupta C, Kurian P, Seva KN, Kalthur SG, D'Souza AS. Amorphological and morphometric study of jugular foramen in dry skulls with its clinical implications. J Craniovertebr Junction Spine. 2014;5:118-121. [Crossref]
15. Das SS, Saluja S, Vasudeva N. Complete morphometric analysis of jugular foramen and its clinical implications. J Craniovertebr Junction Spine. 2016;7:257-264. [Crossref]
16. Matsushima K, Kohno M, Komune N, Miki K, Matsushima T, Rhoton AL Jr. Suprajugular extension of the retrosigmoid approach: microsurgical anatomy. J Neurosurg. 2014;121:397-407. [Crossref]

17. Kohno M. [Jugular foramen neurinoma]. In: Kawamoto K, Hongo K, Kurisu K (eds): [Illustrated Brain Tumor Surgery.] Toyko: Igaku-Shoin. 2011:176-179 (In Japanese) [Crossref]
18. Fukuda M, Oishi M, Saito A, Fujii Y. Long-term outcomes after surgical treatment of jugular foramen schwannoma. Skull Base. 2009;19:401-408. [Crossref]
19. Sekerci R, Ogut E, Keles-Celik N. The influences of porus acusticus internus on ethnicity and importance in preoperative and intraoperative approaches. Surg Radiol Anat. 2021;43:1829-1838. [Crossref]
20. Özandaç Polat S, Uygur AG, Öksüzler FY, Öksüzler M, Yücel AH. Morphometric measurements of the internal acoustic meatus. Cukurova Medical Journal. 2019;44:419-426. [Crossref]
21. Akın-Saygin D, Türkoglu FN, Aydın Kabakçı AD, Alpa S. Internal Acoustic Opening: Different Osseous Landmarks and their Clinical Implications. Int J Morphol. 2022;40:1368-1375. [Crossref]
22. Kolagi S, Herur A, Ugale M, Manjula R, Mutalik A. Suboccipital retrosigmoid surgical approach for internal auditory canal - a morphometric anatomical study on dry human temporal bones. Indian J Otolaryngol Head Neck Surg. 2010;62:372-375. [Crossref]
23. Bozbuğa M, Öztürk A, Arı Z, Sahinoglu K, Bayraktar B, Polat G, Gurel I. Surgical anatomy of the temporal bone and measurements of the skull base for transpetrosal approach. Okajimas Folia Anat Jpn.1998;75:33-39. [Crossref]
24. Day JD, Jordi XK, Fukushima T, Giannota S. Microsurgical anatomy of the inner surface of the petrosus bone. Neursurgery. 1994;34:1003-1008. [Crossref]